

Figure 4. Plot of δ_F of the alkali-metal bis(trifluoromethyl)amides, -phosphides, and -arsenides vs δ_F of bis(trifluoromethyl)chalcogenides. Values were taken from ref 26 and 32.

cause deshielding of ^{14}N nuclei.³³ Compared to published ^{14}N chemical shifts of $(\text{CH}_3)_2\text{NLi}^{34}$ and $[(\text{CH}_3)_3\text{Si}]_2\text{NNa}$,³⁵ this effect is observed for $\text{Cs}(\text{CF}_3)_2\text{N}$ (Table II).

Whereas alkali-metal amides are assumed to dissociate in ionizing solvents, alkali-metal phosphides apparently seldom do^{36,37} (excluding complexation with crown ethers³⁸). As an example, $\delta(^{31}\text{P})$ shifts of diphenylphosphides depend on the cation.³⁹ Contrary to this, the ^{31}P chemical shifts of the bis(trifluoromethyl)phosphides are identical within the accuracy of measurement. The very small value of $^2J_{\text{PF}}$ (47.3 Hz) may serve as a further piece of evidence for ionic dissociation of the phosphides.

(33) See ref 25; p 1034.

(34) Webb, G. A. *Annu. Rep. NMR Spectrosc.* **1986**, *18*, 285.

(35) Webb, G. A. *Annu. Rep. NMR Spectrosc.* **1981**, *11B*, 177.

(36) Fluck, E. *Top. Phosphorus Chem.* **1980**, *10*, 193.

(37) Zschunke, A.; Riemer, M.; Krech, F.; Issleib, K. *Phosphorus Sulfur* **1985**, *22*, 349.

(38) Hope, H.; Olmstead, M. M.; Power, Ph. P.; Xu X. *J. Am. Chem. Soc.* **1984**, *106*, 819.

(39) Fluck, E.; Issleib, K. *Z. Naturforsch.* **1965**, *20B*, 1123.

(40) Dyer, J.; Lee, J. *J. Chem. Soc. B.* **1970**, 409.

(41) Packer, K. J. *J. Chem. Soc.* **1963**, 960.

In comparison with phosphines of the type $(\text{CF}_3)_2\text{PY}$ ($\text{Y} = \text{H}, \text{F}, \text{Cl}, \text{Br}, \text{I}$), which give rise to considerably greater values of $^2J_{\text{PF}}$, substantial changes in bonding must be assumed. Burg²⁸ has published values for $^1J_{\text{PC}}$ of the phosphanes $(\text{CF}_3)_2\text{PY}$. $^1J_{\text{PC}}$ increases with increasing polarizability of the Y ligand and reaches a maximum value of 42.8 Hz for $\text{Y} = \text{iodine}$. With respect to the value of 88.0 Hz exhibited by $\text{Na}(\text{CF}_3)_2\text{P}$ and $\text{Cs}(\text{CF}_3)_2\text{P}$, we conclude that the alkali-metal bis(trifluoromethyl)phosphides dissociate in solution.

Conclusion

In this paper we have shown that the alkali-metal bis(trifluoromethyl)amides, -phosphides, and -arsenides are available in a pure form by a one-step reaction. Initial experiments demonstrate their high nucleophilic reactivity. These salts exhibit consistent spectroscopic data not only within the homologues but also in comparison with the isoelectronic bis(trifluoromethyl)chalcogenides.

Addendum

The reaction of $(\text{CF}_3\text{S})_2\text{PH}$ with Na or Cs metal in liquid ammonia, carried out as described in the preparation of alkali-metal bis(trifluoromethyl)phosphides, did not result in the formation of $(\text{CF}_3\text{S})_2\text{PNa}$ but gave high yields of a yellow precipitate that contained all the phosphorus used. It is thought to be highly polymeric.

Acknowledgment. We thank Prof. Dr. T. N. Mitchell for his help in preparing the manuscript.

Registry No. $\text{Cs}(\text{CF}_3)_2\text{N}$, 66566-92-5; CsF , 13400-13-0; $\text{CF}_3\text{N}=\text{CF}_2$, 371-71-1; $\text{CF}_3\text{N}=\text{CFN}(\text{CF}_3)_2$, 686-39-5; $\text{Na}(\text{CF}_3)_2\text{P}$, 119326-83-9; $\text{Cs}(\text{CF}_3)_2\text{P}$, 119326-79-3; Na, 7440-23-5; Cs, 7440-46-2; $(\text{CF}_3)_2\text{PH}$, 460-96-8; $\text{Na}(\text{CF}_3)_2\text{As}$, 119326-84-0; $\text{Cs}(\text{CF}_3)_2\text{As}$, 119326-85-1; $(\text{C}_6\text{H}_5)_2\text{AsH}$, 371-74-4; $(\text{C}_6\text{H}_5)_4\text{As}^+\text{SbCl}_6^-$, 119326-80-6; $\text{K}^+\text{SbCl}_6^-$, 29933-38-8; $(\text{CF}_3\text{S})_2\text{PH}$, 1648-71-1; CsPF_6 , 16893-41-7; CsSbF_6 , 16949-12-5; $(\text{C}_6\text{H}_5)_4\text{As}^+\text{SbF}_6^-$, 30185-61-6; $(\text{C}_2\text{H}_5)_4\text{N}^+\text{SbF}_6^-$, 4455-34-9; $(\text{C}_6\text{H}_5)_4\text{As}^+(\text{CF}_3)_2\text{N}^-$, 119326-81-7; $(\text{C}_2\text{H}_5)_4\text{N}^+(\text{CF}_3)_2\text{N}^-$, 119326-82-8; $\text{CF}_3\text{P}=\text{CF}_2$, 72344-34-4; CH_3I , 74-88-4; $\text{CH}_3\text{P}(\text{CF}_3)_2$, 1605-54-5.

Contribution from the Department of Chemistry, Texas A&M University, College Station, Texas 77843

Spectroscopic and Chemical Studies of Nickel(II) Hydrides

Marcetta Y. Darensbourg,* Maria Ludwig, and Charles G. Riordan

Received October 27, 1988

The trans influence of X ligands on the spectroscopic properties of the Ni-H bond is reported for the series of square-planar nickel hydrides *trans*- $\text{HNi}(\text{X})(\text{PCy}_3)_2$ ($\text{X} = \text{Me}, \text{Ph}, \text{CN}, \text{SCN}, \text{I}, \text{Br}, \text{Cl}, \text{SPh}, \text{S}(p\text{-tol}), \text{SH}, \text{OAc}, \text{O}_2\text{CH}, \text{O}_2\text{CPh}, \text{O}_2\text{CCF}_3, \text{OPh}$) prepared by oxidative addition of HX to $[\text{Ni}(\text{PCy}_3)_2]_2\text{N}_2$ or derivatives of subsequent products. The infrared-derived parameter $\nu(\text{Ni-H})$ shows a similar ligand dependence as the proton chemical shift of the hydride ligand, with more covalently bound ligands such as methyl or phenyl producing lower $\nu(\text{Ni-H})$ and smaller upfield chemical shifts as compared to those ligands that bind to Ni(II) with more electrostatic character such as anionic O-donor ligands. Comparisons with other ligand influenced, spectroscopic scales are made. Carbon dioxide and iodomethane were used as chemical probes of reactivity at the Ni-X or Ni-H bond. The derivatives with stronger Ni-H bonds (S and O donors) show no reactivity at the hydride while the C-bond derivatives exhibit CO_2 insertion at the hydride. The Ni-H functionality is active toward iodomethane in the C-donor derivatives. A mechanism of hydrogen atom abstraction by methyl radicals is consistent with literature precedents as well as the Ni-H bond strengths determined by spectroscopies.

Introduction

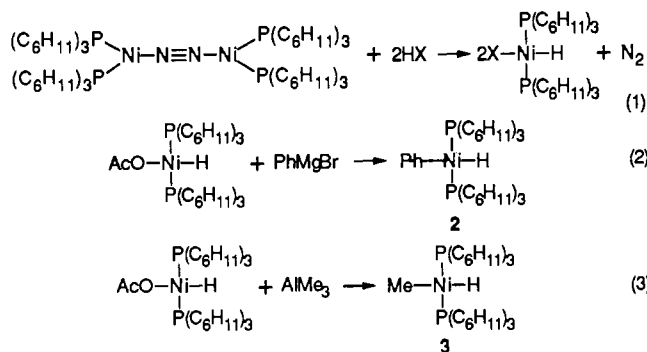
A broad series of square-planar nickel(II) hydrides, *trans*- $\text{HNi}(\text{X})\text{P}(\text{C}_6\text{H}_{11})_3)_2$, is accessible from the dinitrogen complex¹ (eq 1) or derivatives of subsequent products (eq 2 and 3) as

reported^{2,3} for $\text{X} = \text{CH}_3, \text{C}_6\text{H}_5, \text{OAc}, \text{CN}, \text{SCN}, \text{I}, \text{Br}, \text{Cl}, \text{OC}_6\text{H}_5, \text{S}(p\text{-C}_6\text{H}_4\text{CH}_3)$, and SC_6H_5 and extended in our laboratories to include SH, O_2CH , $\text{O}_2\text{CC}_6\text{H}_5$, and O_2CCF_3 . This series provides

(2) Jonas, K.; Wilke, G. *Angew. Chem., Int. Ed. Engl.* **1969**, *8*, 519.

(3) (a) Green, M. L. H.; Saito, T. *J. Chem. Soc., Chem. Commun.* **1969**, 208. (b) Green, M. L. H.; Saito, T.; Tanfield, P. J. *J. Chem. Soc. A* **1971**, 152. (c) Osakada, K.; Hayashi, H.; Maeda, M.; Yamamoto, Y.; Yamamoto, A. *Chem. Lett.* **1986**, 597.

(1) (a) Jolly, P. W.; Jonas, K. *Angew. Chem., Int. Ed. Engl.* **1968**, *7*, 731. (b) Jolly, P. W.; Jonas, K.; Kruger, C.; Tsay, Y.-H. *J. Organomet. Chem.* **1971**, *33*, 109.



the opportunity to examine the relative reactivities of X and H ligands, preliminary studies of which were recently reported.⁴ The organometallic derivative **2** reacts with CO₂ yielding the formate insertion product, whereas the analogous hydrido-methyl complex **3** underwent a rather complicated reaction as evidenced in Scheme I.

Given the importance of the nickel hydride functional group in industrial⁵ and possibly enzymatic⁶ catalysis and the limited number of well-defined studies of the effect of trans ligands on either spectroscopic properties or reactivity of the hydride ligand, we have determined NMR and infrared parameters of the *trans*-HNi(X)(PCy₃)₂ complexes. The results are, in general, in agreement with those obtained for the analogous platinum hydride series *trans*-HPt(X)(PEt₃)₂.⁷ The differences, as will be seen below, lie in the sensitivity with which the lighter metal transmits electronic information to the hydride and in the breadth of the series.

Experimental Section

Materials and Methods. All manipulations were performed by using standard Schlenk techniques or in an argon-atmosphere glovebox. Tetrahydrofuran, benzene, and toluene were distilled from sodium benzophenone ketyl under nitrogen. Diethyl ether was distilled from LiAlH₄ under nitrogen. All other reagents were purchased as reagent grade or better from standard vendors and used without further purification. Infrared spectra were recorded on an IBM FTIR/85 or FTIR/32 instrument using 0.10-mm CaF₂ solution cells or KBr pellets. ¹H, ²H, ¹³C, and ³¹P NMR spectra were obtained on a Model XL200 Varian spectrometer. ³¹P NMR spectra were referenced against H₃PO₄, and other nuclei were referenced against TMS. GC/MS analyses were obtained on a high-resolution VG Analytical Ltd. 70-S mass spectrometer equipped with a DS 11/250 J data system. A Carboxphere-packed column was used in the GC, under isothermal conditions (175 °C); the GC was connected to the MS with a jet separator interface. Scanning conditions were at 1 s/decade over the mass range of 10–300. The instrument was operated at 17 eV. Elemental analyses were performed by Galbraith Laboratories, Inc., Knoxville, TN.

[Ni(PCy₃)₂]₂N₂. The starting material was prepared according to the method of Jonas and Jolly.¹ To a suspension of Ni(acac)₂ (5.0 g, 19.5 mmol) and PCy₃ (11 g, 39 mmol) in 30 mL of toluene at –20 °C was added Al(CH₃)₃ in toluene (2.0 M, 19 mL) dropwise over 1.5 h. The resulting red-brown solution was allowed to warm to room temperature and stirred under a nitrogen stream for 30 h. The mixture was cooled to –78 °C for 1 h and filtered to isolate a deep red solid product that was washed with ether (3 × 5 mL): yield 54%; IR (KBr) ν(NN) 2038 cm⁻¹; ¹H NMR (C₆D₆) δ 2.2 (m), δ 1.7 (m), δ 1.3 (m); ³¹P NMR (C₆D₆) δ 47.3.

HNi(O₂CR)(PCy₃)₂ (R = CH₃ (**1a**),² H (**1b**), C₆H₅ (**1c**), CF₃ (**1d**)). These new carboxylic acid derivatives, **1b–d**, were synthesized in a fashion analogous to that for **1a** reported by Jonas and Wilke.² In a typical reaction, argon was purged through a solution of [Ni(PCy₃)₂]₂N₂ (3.0 g, 2.4 mmol) in 40 mL of toluene for 1 h. The resulting orange solution was concentrated to 10 mL. A slight excess (5.2 mmol) of the appropriate acid in 25 mL of ether was added. The resulting yellow precipitate was filtered, washed with ether (2 × 5 mL), and dried in

Scheme I. CO₂ Insertion Reactions with HNi(R)(PCy₃)₂ (R = Ph, Me)

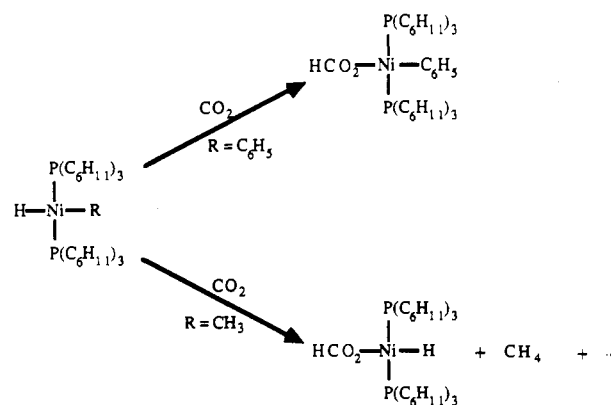


Table I. Spectral Data for *trans*-HNi(X)(PCy₃)₂ Complexes

X	δ(Ni–H), ^a ppm	J(PH), Hz	δ(P), ^b ppm	ν(Ni–H), ^c cm ⁻¹
Ph	–14.8	66.0	38.8	1805
Me	–15.1	68.5	44.3	1807, 1800
CN	–15.3	64.5		1870
S(<i>p</i> -tol)	–19.9	72.0	36.2	1932
SPH	–19.9	72.0	36.1	1929
SH	–18.7	69.0	36.8	1904
I	–20.1	71.9		1976
Br	–22.9	72.8		1917
SCN	–23.5	72.9		1928
Cl	–24.4	73.8		1916, 1900
O ₂ CPh	–27.5	75.9	33.7	1960
O ₂ CH	–27.6	76.7	33.0	1931
OAc	–27.7	77.0	33.1	1925, 1920
OPh	–27.9	76.6	30.9	1946, 1940
O ₂ CCF ₃	–28.0	75.1	33.1	1944

^a C₆D₆ solvent; peak is a triplet. ^b C₆D₆, H₃PO₄ external standard. ^c KBr pellet.

vacuo. Spectroscopic data are contained in Table I. Additional data are as follows. **1a**: yield 81%; IR(KBr) ν(CO) 1618 cm⁻¹; ¹H NMR (C₆D₆) δ 8.9 (HCO₂Ni). **1c**: yield 60%; IR(KBr) ν(CO) 1617 cm⁻¹. **1d**: yield 49%; IR(KBr) ν(CO) 1698 cm⁻¹. Anal. Found (calcd) for **1b** (C₃₇H₆₈NiO₂P₂): C, 61.91 (66.77); H, 9.71 (10.3); P, 8.69 (9.31). **1c** (C₄₃H₇₂NiO₂P₂): C, 66.43 (69.63); H, 9.65 (9.78); P, 8.32 (8.35). **1d** (C₃₄F₃H₆₇NiO₂P₂): C, 60.6 (62.2); H, 9.24 (9.21); P, 8.22 (8.44).

HNi(R)(PCy₃)₂ (R = C₆H₅ (**2**), CH₃ (**3**)). These light- and heat-sensitive compounds were synthesized with modifications, according to Jonas and Wilke.² **1a** (2.3 g, 3.4 mmol) in 40 mL of toluene was placed in a foil-covered flask and cooled to –30 °C. In the case of **2**, PhMgBr (1.2 mL, 3.0 M) in toluene was added, or for **3**, Al(CH₃)₃ (1.7 mL, 2.0 M) in toluene was added. The resulting solution was stirred while slowly being warmed to room temperature. The volume was reduced to 5 mL in vacuo and 25 mL of ether was added. The yellow product was subsequently filtered and dried in vacuo. Yields: for **2**, 49%; for **3**, 74%. Spectroscopic data are contained in Table I. Additional data for **2**: ¹H NMR (C₆D₆) δ –0.30 (d of t, J(P–CH) = 6.1 Hz, J(HNi–CH) = 1.6 Hz).

HNi(SR)(PCy₃)₂ (R = H (**4a**), C₆H₅ (**4b**), *p*-C₆H₄CH₃ (**4c**)). In a typical preparation argon was purged through a solution of [Ni(PCy₃)₂]₂N₂ (6.3 g, 5.0 mmol) in 50 mL of toluene for 1 h. The resulting orange solution was concentrated to 10 mL and cooled to –10 °C. The appropriate acid, RSH (2 equiv), was added in 30 mL of ether resulting in the formation of a yellow-brown suspension. The mixture was allowed to reach room temperature while stirring and then cooled to –78 °C before filtering. The product was washed with ether (2 × 5 mL) and dried in vacuo. Spectroscopic data are contained in Table I. Yields: for **4a**, 30%; for **4b**, 60%; for **4c**, 67%.

HNi(OC₆H₅)(PCy₃)₂ (**5**). This compound was reported by Jonas and Wilke² without details of its synthesis. It was prepared in our laboratories in a manner similar to that for **1a**, but C₆H₅OH was used in place of CH₃COOH: yield 55%; IR (KBr) ν(C=C) 1585, 1486 cm⁻¹. Anal. Found (calcd) for C₄₂H₇₂NiO₂P₂: C, 69.29 (70.7); H, 9.98 (10.1); P, 9.03 (8.69); Ni, 8.23 (8.23).

Reactions of 1a–d, 4b, 4c, and 5 with Carbon Dioxide. In a typical reaction 0.030 mmol of the nickel hydride was dissolved in C₆D₆ (0.5 mL)

(4) Darensbourg, D. J.; Darensbourg, M. Y.; Goh, L. Y.; Ludwig, M.; Wiegrefe, P. *J. Am. Chem. Soc.* **1987**, *109*, 7539.

(5) Tolman, C. A. *J. Am. Chem. Soc.* **1970**, *92*, 6777.

(6) Crabtree, R. H. *Inorg. Chim. Acta* **1986**, *125*, L7 and references therein.

(7) (a) Atkins, P. W.; Green, J. C.; Green, M. L. H. *J. Chem. Soc. A* **1968**, 2275. (b) Chatt, J.; Shaw, B. L. *J. Chem. Soc.* **1962**, 5075. (c) Dean, R. R.; Green, J. C. *J. Chem. Soc. A* **1968**, 3047.

Table II. Product Distribution from Isotopic Labeling Experiments

entry	reactants ^a	product distribn						
		methane ^b				ethane ^b		
		CH ₄	CH ₃ D	CD ₃ H	CD ₄	C ₂ H ₆	CH ₃ CD ₃	C ₂ D ₆
1	HNiMe(PCy ₃) ₂ /CD ₃ I	2.0	0	1.0	0	1.0	2.8	1.2
2	DNiMe(PCy ₃) ₂ /CH ₃ I	1.0	5.0	1.0	0	1.0	0	0
3	DNiMe(PCy ₃) ₂ /CD ₃ I	1.1	1.8	1.0	1.7	1.0	2.8	1.7

^aReactions were carried out in the absence of light in toluene. ^bRelative ratios of the labeled methane and ethane products, respectively. The overall methane/ethane ratio was 1.0/1.8 for all entries.

in a 5-mm NMR tube. A partial vacuum was pulled on the sample and the tube subsequently backfilled with an atmosphere of CO₂. No reaction was seen after 24 h as monitored by ¹H NMR. The nickel formate derivative exchanges CO₂ with an atmosphere of ¹³CO₂, but the other carboxylic derivatives do not.⁴ The reactions of **2** and **3** with CO₂ have been previously published by this group.⁴

Reactions of 1a-c, 4b, and 4c with Iodomethane. In a typical reaction 0.020 mmol of the nickel hydride was dissolved in C₆D₆ (0.5 mL) in a 5-mm NMR tube. One molar equivalent (0.020 mmol) of MeI was added via a microliter syringe. As the hydride resonance for the starting material disappeared, a new hydride signal for HNi(I)(PCy₃)₂ grew in. The organic products were also seen in the spectra. Yields based on ¹H NMR were as follows: **1a**, 72%; **1b**, 80%; **1c**, 60%; **4b**, 85%; **4c**, 96%.

Reactions of 3 with Iodomethane. All of the following reactions were carried out in the dark. To a solution of **3** (18 mg, 0.028 mmol) in C₆D₆ (0.5 mL) was added MeI (0.002 mL, 0.032 mmol). The sole nickel-containing product detected was HNi(I)(PCy₃)₂ in low (17%) yield. A similar reaction employing 10 molar equiv of MeI increased the HNi(I)(PCy₃)₂ yield to 71%. In both cases methane and ethane were detected by GC in the same relative ratio (1:1.8). Similar reactions were carried out on toluene solutions of **3** (28 mg, 0.044 mmol) and its deuterated analogue DNi(CH₃)(PCy₃)₂ by addition of 1 molar equiv of CD₃I or CH₃I. The results of the GC/MS analyses on the gases over the solutions are listed in Table II.

Results

A triplet in the high-field region of the ¹H NMR is seen for all of the nickel(II) hydrides examined in this study, indicating an identical ligation sphere for all compounds. Despite their steric bulk, two PCy₃ ligands remain bound to the nickel in all cases examined. The compounds are all air-sensitive, yellow solids. The methyl and phenyl derivatives are light-sensitive even in the solid state, producing methane and benzene, respectively, upon photolytic decomposition.

Table I lists nickel hydride ¹H NMR chemical shifts, ³¹P[¹H] NMR chemical shifts, phosphorous-hydrogen coupling constants, and nickel-hydrogen stretching frequencies for a range of X substituents. The Ni-H stretching frequency ranges from 1805 to 1976 cm⁻¹, and was verified as such for the acetate, formate, and methyl derivatives by deuterium incorporation. The deuterium analogues were prepared by mixing the appropriate acid precursor reagent with a large molar excess of D₂O. The monodeuterated acid was subsequently reacted with [Ni(PCy₃)₂]₂N₂, analogous to the procedures in the Experimental Section for these complexes. Greater than 90% deuterium incorporation was indicated by ¹H and ²H NMR spectra. The ν(Ni-D) bands were not located at their calculated positions (1300-1365 cm⁻¹) due to masking by other ligand bands. Hydride chemical shift values, upfield from TMS, range from -15 ppm for the phenyl derivative to -28 ppm for the trifluoroacetate derivative. The ordering of hydride chemical shifts follows similarly, but not precisely, the trans influence series based on Pt(II) complexes.⁸ We choose to classify the X ligands into categories according to the donor trans to the hydride: carbon-bound ligands, approximately -15 ppm; halides and pseudohalides, -20 to -25 ppm; oxygen donors, -27 to -28 ppm. Consistent with this, the range of Ni-H stretching frequencies can also be classified into subgroups. With carbon-bound ligands the values are in the 1805-1870-cm⁻¹ range, halides and pseudohalides, 1910 to 1976 cm⁻¹-range, and oxygen donors,

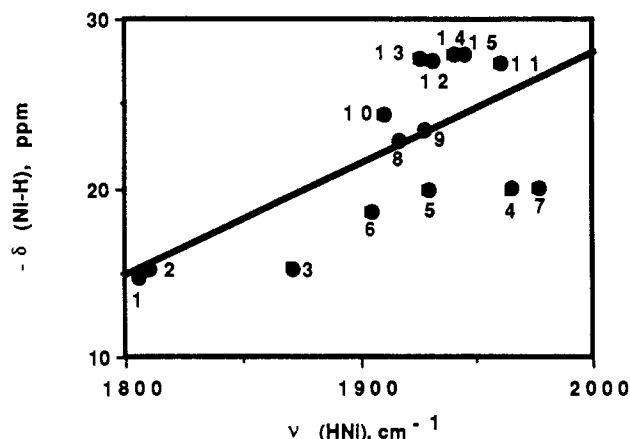


Figure 1. Plot of $-\delta(\text{Ni-H})$ vs $\nu(\text{Ni-H})$ for *trans*-HNi(X)(PCy₃)₂. X is Ph (1), Me (2), CN (3), *S*(*p*-tol) (4), SPh (5), SH (6), I (7), Br (8), SCN (9), Cl (10), PhCO₂ (11), HCO₂ (12), AcO (13), PhO (14), and CF₃CO₂ (15).

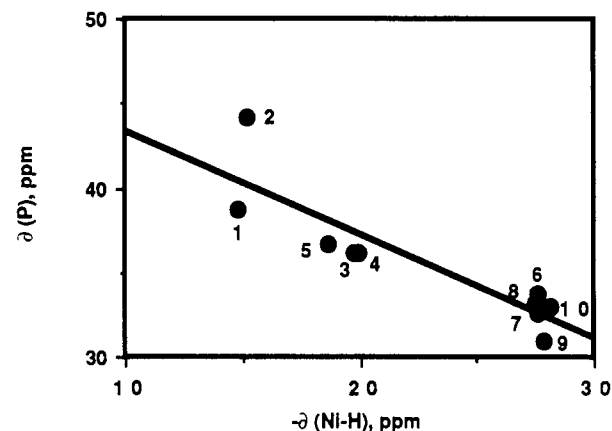


Figure 2. Plot of $\delta(\text{P})$ vs $-\delta(\text{Ni-H})$ for *trans*-HNi(X)(PCy₃)₂. X is Ph (1), Me (2), *S*(*p*-tol) (3), SPh (4), SH (5), PhCO₂ (6), HCO₂ (7), AcO (8), PhO (9), and CF₃CO₂ (10).

1925-1960-cm⁻¹ range. A graphical representation of the correlation between Ni-H stretching frequency and hydride chemical shift values is shown in Figure 1.

The ³¹P[¹H] NMR spectra for these complexes exhibit a single resonance indicating a trans disposition of phosphine ligands. The ³¹P chemical shift values, referenced against H₃PO₄, range from 44 ppm for the methyl derivative to 31 ppm for the phenolate derivative. In the 36-44 ppm range, the carbon- and sulfur-bound complexes have phosphorus chemical shifts further downfield than those of the oxygen-bound derivatives. These broad groupings shows a trend similar to the hydride ¹H NMR chemical shift values, and this correlation is shown in Figure 2. The phosphorus-hydrogen coupling constants range from 64 to 77 Hz, and may also be grouped into categories: carbon-bound ligands, 63-68 Hz; halides and pseudohalides, 72-74 Hz; oxygen-bound ligands, 75-77 Hz. Figure 3 depicts the good correlation between *J*(PH) and the hydride chemical shift.

Carbon dioxide and iodomethane were used as probes for relative reactivity for the Ni-H and Ni-X bonds. Carbon dioxide reacts cleanly with **2** at the hydride to produce the formate product

(8) Cotton, F. A.; Wilkinson, G. *Advanced Inorganic Chemistry*, 5th ed.; John Wiley and Sons: New York, 1988.

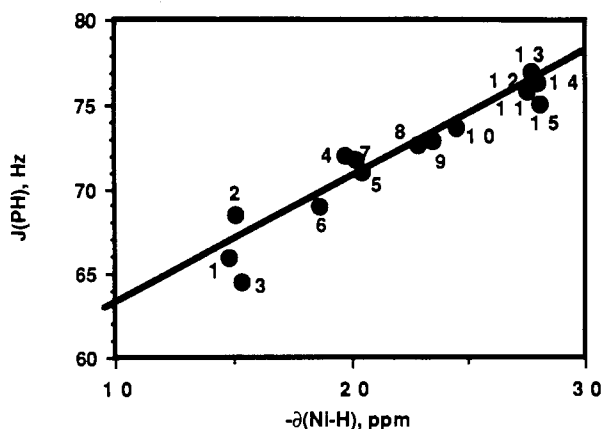
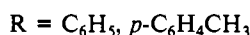
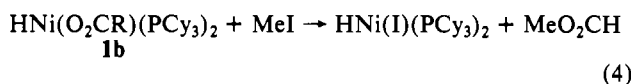


Figure 3. Plot of $J(\text{PH})$ vs $-\delta(\text{Ni-H})$ for $\text{trans-HNi}(\text{X})(\text{PCy}_3)_2$. X is Ph (1), Me (2), CN (3), S(*p*-tol) (4), SPh (5), SH (6), I (7), Br (8), SCN (9), Cl (10), PhCO₂ (11), HCO₂ (12), AcO (13), PhO (14), and CF₃CO₂ (15).

with no insertion into the nickel-carbon bond.⁴ Carbon dioxide reacts with **3** to form several nickel-containing species, the only isolable one being **1b**. However spectroscopic evidence suggests the straightforward formate insertion product is formed in small yields.⁴ Carbon dioxide does not react with any of the non-carbon-bound derivatives in the series. Iodomethane reacts, nearly quantitatively, at the X ligands which have accessible lone pairs of electrons (eq 4 and 5).



Methyl iodide exhibits several reaction pathways including radical reactions with the carbon-bound derivatives of this series. Methane and ethane are the organic products of reaction of MeI with $\text{HNi}(\text{CH}_3)(\text{PCy}_3)_2$ (**3**). A small amount (14%) of $\text{HNi}(\text{I})(\text{PCy}_3)_2$ was the only spectroscopically identified Ni-containing product. The results of labeling studies employed to elucidate the source of organic products are listed in Table II. Since **3** is stable toward CH₄ elimination in the dark, its rapid production in the presence of MeI (entry 1) suggests interaction of MeI at the metal, perhaps promoting oxidation to Ni(I) and subsequent reductive elimination⁹ or yielding a 5-coordinate species that facilitates reductive elimination from **3**.¹⁰ However, production of CH₃D and CH₃CD₃ in entry 1 indicates MeI also interacts with the NiH and NiMe bonds, respectively. The ethane isotopomers detected in entries 1 and 3 point to radical behavior in the reaction; perdeuterioethane can only be produced from coupling of CD₃• radicals of CD₃I. Similarly, C₂H₆ results from coupling of CH₃• radicals of the organometallic reactant.

Discussion

To a reasonable approximation, in the absence of extensive coupling to other vibrational modes, nickel-hydrogen stretching frequencies in these complexes are proportional to their force constants¹¹ (Table III) and hence to bond strengths. The ligands

Table III. Comparison of Force Constants in $\text{trans-HM}(\text{X})(\text{PR}_3)_2$ (M = Pt, R = Et; M = Ni, R = Cy)

M	X	$\nu(\text{M-H}), \text{cm}^{-1}$	$10^{-3}k, \text{mdyn } \text{Å}^{-1}$
Ni	Ph	1805	1.28
Ni	Me	1807	1.28
Ni	CN	1870	1.37
Ni	S(<i>p</i> -tol)	1932	1.46
Ni	SPh	1929	1.46
Ni	SH	1904	1.43
Ni	I	1976	1.53
Ni	Br	1917	1.44
Ni	SCN	1928	1.46
Ni	Cl	1916	1.44
Ni	PhCO ₂	1960	1.51
Ni	HCO ₂	1931	1.46
Ni	CH ₃ CO ₂	1925	1.45
Ni	PhO	1946	1.46
Ni	CF ₃ CO ₂	1944	1.48
Pt	CN	2072 ^a	1.71
Pt	SCN	2112 ^a	1.90
Pt	Cl	2183 ^a	1.96
Pt	Br	2220 ^a	2.00
Pt	NO ₃	2242 ^a	2.02
Pt	CF ₃ CO ₂	2258 ^b	2.03

^aChatt, J.; Shaw, B. L. *J. Chem. Soc.* **1962**, 5075. ^bAtkins, P. W.; Green, J. C.; Green, M. L. H. *J. Chem. Soc. A* **1968**, 2275.

bound trans to the hydride which produce stronger nickel-hydrogen bonds are those with donor atoms of high electronegativity, or, energetically, with stable, low-lying HOMO's, i.e., hard donor sites.

Metal-hydrogen chemical shifts are, in general, highly metal and coordination sphere dependent. Absolute values are not usefully transferred from one metal system to another. However, within a similar series of complexes, maintaining metal, oxidation state, and coordination geometry constant, hydride chemical shifts may be interpreted with some confidence. Upfield chemical shifts indicate greater electronic shielding of the hydrogen, which suggests stronger bonding or a hydrogen that is "buried" in the metal's electron cloud. Again, ligands with hard donor sites trans to the hydride permit the hydrogen greater access to the electron density on the nickel. In contrast, when the X ligand is capable of covalent bonding to the metal, like the carbon-bound ligands, the hydride competes less successfully. While both IR and ¹H NMR spectroscopies show analogous trends in bonding, $\delta(\text{Ni-H})$ is insensitive to the electronic nature of substituents on the donor ligand while $\nu(\text{Ni-H})$ appears to be more sensitive to the X ligand as a whole.

That phosphorus ligands cis to the hydride are also subject to electronic changes on Ni as X varies is evidenced in the $\delta(\text{P})$. A trend in resonance position similar to that for the hydride chemical shifts is seen. Apparently complexes with more shielded hydrides have nickel-phosphorus bonding that is more covalent, as evidenced by the upfield $\delta(\text{P})$. The communication between the hydride and the phosphorus ligands is supported in the $J(\text{PH})$. An excellent correlation exists between the hydride chemical shift and $J(\text{PH})$. The hydrides that are more "buried" in the nickel display larger coupling to the phosphorus ligands.

In general, the trend in trans influence of X donor ligands on hydrides, in our series, agrees with the spectroscopic results of the series of platinum(II) hydrides $\text{trans-HPt}(\text{X})(\text{PEt}_3)_2$ studied by several workers.⁷ Energy-factored force constants derived from $\nu(\text{M-H})$ suggest the platinum-hydrogen bonds are stronger (Table III) than the analogous nickel-hydrogen bonds. However, while the correlation between hydride chemical shift and phosphorus-hydrogen coupling for the nickel series is excellent, no correlation is seen in the platinum series. Since scalar coupling occurs primarily via an s-orbital mechanism, the smaller nickel 4s orbital is more sensitive to its ligation sphere than the more diffuse platinum 5s orbital.

(9) An EPR spectrum of the reaction of **3** with MeI was obtained at 77 K. The spectrum was similar to that of $\text{NiI}(\text{PCy}_3)_2$ taken under similar experimental conditions (Heimbach, P. *Angew. Chem., Int. Ed. Engl.* **1964**, *3*, 648). Darenbourg, M. Y.; Ludwig, M. Unpublished results.

(10) The addition of ligands such as CO promote the reductive elimination of CH₄ from **3**.

(11) $\Delta E = h/2\pi(k/\mu)^{1/2}$.

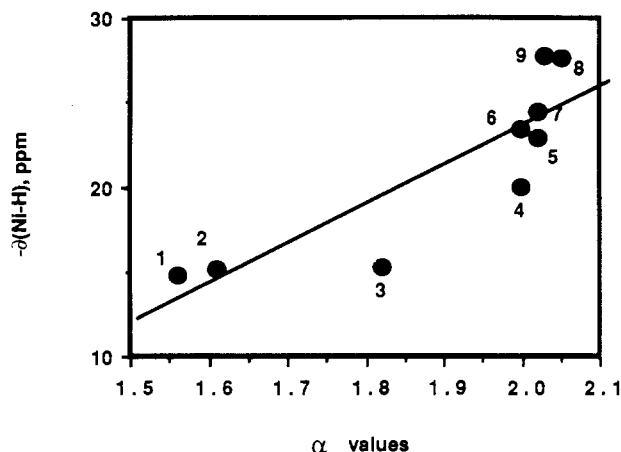


Figure 4. Plot of $-\delta(\text{Ni-H})$ vs α values¹⁴ for $\text{trans-HNi(X)(PCy}_3)_2$. X is Ph (1), Me (2), CN (3), I (4), Br (5), SCN (6), Cl (7), HCO_2 (8), and AcO (9).

Spectroscopic scales have been developed for other complex geometries. Marzilli tabulated (as τ values) the chemical shifts of the α -proton of the *tert*-butylpyridine ligand trans to the substituents, X, in the Co(III) complexes $\text{LCo(DH)}_2\text{X}$ (L = 4-*tert*-butylpyridine and DH = $\text{HONC(CH}_3)_2\text{C(CH}_3)_2\text{NO}^-$) and reported these spectroscopic substituent constants as a proton NMR spectrochemical series.¹² Smaller α values were noted for

(12) Marzilli, L. G.; Politzer, P.; Trogler, W. C.; Stewart, R. C. *Inorg. Chem.* **1975**, *14*, 2389.

soft carbon-donor ligands, and values increased with the hardness of the substituent: Ph ($\alpha = 1.56$) < CH_3 (1.61) < SCN (1.96) < I (2.00) < Cl, Br (2.02) < OAc (2.03) < F (2.24). The transferability was shown in that the α -values correlate with the platinum-hydrogen stretching frequency in $\text{trans-HPt(X)}_2\text{L}_2$ and the Pt-C-H coupling constant in $\text{trans-Pt(CH}_3\text{)(X)L}_2$.¹³ A plot of Marzilli's α values vs nickel-hydride chemical shifts of our series (Figure 4) further supports the transferability of such substituent constants. It is interesting to note that the same trends exist in coordination complexes of Co(III) and the "softer" coordination sphere of the nickel(II) and platinum(II) phosphines studied in other laboratories.

The wide range of nickel-hydrogen bond strengths is evidenced by reactivity with MeI and CO_2 . Both react with carbon-bound derivatives preferentially at the hydride ligand. The sulfur- and oxygen-bound derivatives show no reactivity at the hydride. Iodomethane reacts preferentially at the ligands with easily accessible lone pairs, alkylating the ligand and leaving the hydride intact. Carbon dioxide shows no reactivity with the sulfur and oxygen derivatives at either the NiH or NiX sites.¹⁴

Acknowledgment. The financial support of the Robert A. Welch Foundation is greatly appreciated. In addition, we acknowledge Lai Y. Goh's assistance in our initial syntheses and the helpful comments of D. J. Darensbourg.

(13) Appleton, T. G.; Clark, H. C.; Manzer, L. E. *Coord. Chem. Rev.* **1973**, *10*, 335.

(14) (a) Newman, L. J.; Bergman, R. G. *J. Am. Chem. Soc.* **1985**, *107*, 5314. (b) No reaction of **5** with CO_2 was observed even under 1000 psi of CO_2 ; Darensbourg, D. J.; Wiegrefe, P. W. Unpublished results.

Contribution from the Department of Chemical Engineering, The Pennsylvania State University, University Park, Pennsylvania 16802

DRIFTS Investigation of the Decomposition of Ruthenium Clusters on Carbon and the Subsequent Ruthenium/Carbon Catalysts

Jeremy J. Venter and M. Albert Vannice*

Received August 5, 1988

The thermal decomposition of $\text{Ru}_3(\text{CO})_{12}$ has been studied for the first time by dispersing this cluster on an oxygen-free carbon support and using diffuse reflectance infrared Fourier transform spectroscopy (DRIFTS). The $\text{Ru}_3(\text{CO})_{12}$ clusters on carbon decomposed straightforwardly in He but transformed to $\text{H}_4\text{Ru}_4(\text{CO})_{12}$ during decarbonylation in H_2 . First-order rate constants of decomposition in He and H_2 were determined for each cluster, compared to literature values for nucleophilic substitution in solution, and found to be similar. This implies that the rate-determining step in these decomposition reactions appears to be the same as that in substitution reactions—removal of the first CO ligand. The activation energy of decarbonylation of $\text{Ru}_3(\text{CO})_{12}$ was near 20.5 kcal/mol in He, while $\text{Ru}_3(\text{CO})_{12}$ and $\text{H}_4\text{Ru}_4(\text{CO})_{12}$ had values of 18–22 kcal/mol in H_2 . These activation energies are lower than those observed for substitution reactions in solution, but this can be explained by considering Ru–Ru bond formation during the decomposition process to give highly dispersed metallic Ru crystallites. Chemisorption measurements confirmed the presence of very small Ru particles on carbon following decomposition at 673 K under either He or H_2 , and the DRIFTS spectra of CO chemisorbed on these Ru crystallites indicated the presence of zerovalent Ru. The resulting Ru/C catalysts exhibited low CO hydrogenation turnover frequencies consistent with values in the literature for very small Ru crystallites on inert supports. The isothermal, integral heat of adsorption of CO was measured calorimetrically at 300 K and found to be 24.2 ± 1.6 kcal/mol. This study is part of the first successful application of an IR spectroscopic technique to characterize carbon-supported metals.

Introduction

A significant interest in carbon as a support for metal catalysts presently exists,^{1–16} primarily because amorphous carbons can be prepared with high surface areas of over 1000 m^2/g and can stabilize highly dispersed Ru, Co, Fe, and Mn particles.^{1–7} These carbons can be highly dehydroxylated and decarboxylated, and they possess the capability to stabilize highly dispersed crystallites in metallic form in the absence of surface functional groups which are typically present on ordinary oxide supports.¹⁷ These highly dispersed metals have been shown to be very active and, in some

cases, quite unique CO hydrogenation catalysts.^{1–7} Electronic interactions in these metal-carbon systems have been pro-

(1) Jung, H. J.; Vannice, M. A.; Mulay, L. N.; Stanfield, R. M.; Delgass, W. N. *J. Catal.* **1982**, *76*, 208.

(2) Niemantsverdriet, J. W.; van der Kraan, A. M.; Delgass, W. N.; Vannice, M. A. *J. Phys. Chem.* **1985**, *89*, 67.

(3) Kaminsky, M.; Yoon, K. J.; Geoffroy, G. L.; Vannice, M. A. *J. Catal.* **1985**, *91*, 338.

(4) Chen, A.; Kaminsky, M.; Geoffroy, G. L.; Vannice, M. A. *J. Phys. Chem.* **1986**, *90*, 4810.

(5) Venter, J. J.; Kaminsky, M.; Geoffroy, G. L.; Vannice, M. A. *J. Catal.* **1987**, *103*, 450.

(6) Venter, J. J.; Kaminsky, M.; Geoffroy, G. L.; Vannice, M. A. *J. Catal.* **1987**, *105*, 155.

* To whom correspondence should be sent.